

Intrinsic Band Gap and Electrically Tunable Flat Bands in Twisted Double Bilayer Graphene

Young Woo Choi and Hyoungh Joon Choi*

Department of Physics, Yonsei University, Seoul 03722, Korea

(Dated: March 5, 2019)

We present atomistic calculations on structural and electronic properties of twisted double bilayer graphene (TDBG) consisting of two sets of rotationally misaligned Bernal-stacked bilayer graphene. Obtained equilibrium atomic structures exhibit in-plane strains and the modulation of the interlayer distances at the rotationally mismatched interface layers. We find that the electronic structure of TDBG can have an intrinsic band gap at the charge neutral point for a large range of the twist angle θ . Near $\theta = 1.25^\circ$, the intrinsic band gap disappears and TDBG hosts flat bands at the Fermi level that are energetically well separated from higher and lower energy bands. We also show that the flat bands are easily tunable by applying vertical electric fields, and extremely narrow bandwidths less than 10 meV can be achieved for the electron-side flat bands in a wide range of the twist angle. Our results serve as a theoretical guide for exploring emergent correlated electron physics in this versatile moiré superlattice system.

Moiré superlattices in two-dimensional van der Waals heterostructures have become a new experimental platform for studying correlated electron physics, featuring various degrees of freedom that can be externally controlled. In the case of twisted bilayer graphene (TBG), bandwidths of Dirac electrons in graphene are tunable through the fine control of the twist angle [1–3] and flat bands emerge near so-called magic angles. Recent series of experiments have shown that such magic-angle twisted bilayer graphene (MA-TBG) hosts correlated insulating states at the half fillings of the flat bands and superconductivity upon doping additional electrons or holes near the insulating phases [4, 5]. These observations have established that the magic-angle twisted bilayer graphene is a promising platform for exploring correlated electron physics.

Furthermore, MA-TBG has a great advantage in terms of tunability because it is possible to explore the correlated phases at different doping levels with a single device, owing to the electrical controllability of the carrier concentration. In addition, the necessity of the fine control of the twist angle can be further relaxed by application of hydrostatic pressure to TBG samples. It has been theoretically suggested that the interlayer coupling in TBG can be enhanced by applying pressure, inducing flat bands in a large range of the twist angle rather than at certain discrete magic angles [6, 7]. Furthermore, a recent experimental work has shown that, by applying pressure, the correlated insulating states and superconductivity are induced at a twist angle larger than the magic angle, where the correlated phases are absent without the pressure [8].

So far limited attention has been paid to the layer-number degree of freedom. Since the number of layers is an important degree of freedom that strongly affects physical properties of van der Waals materials, it can also provide an additional dimension to the flat-band physics in moiré superlattices. In particular, AB-stacked bilayer

graphene (AB-BLG) has a widely tunable band gap that can be controlled by a vertical electric field [9–11]. Therefore, one can expect that a moiré superlattice formed by two sets of AB-BLG inherits such tunability of the electronic structure with an external bias, as in continuum models [12, 13].

In this work, we present an atomistic study on the electronic structure of twisted double bilayer graphene (TDBG) consisting of two sets of AB-stacked bilayer graphene with a twist. Considering both in and out of plane structural relaxations, we calculate the electronic structure of TDBG at small twist angles and discuss the similarities and differences with TBG. We find that TDBG has an intrinsic band gap at the charge neutral point over a large range of the twist angle, owing to the absence of the inversion symmetry. We also show that TDBG hosts flat bands near the Fermi level at small twist angles similar to TBG, but their bandwidths can be further tuned by a moderate vertical electric field. As a result, we predict that extremely narrow bandwidths less than 10 meV can be achieved for a large range of the twist angle.

The commensurate moiré supercell of twisted double bilayer graphene is constructed by stacking a rotated AB-stacked bilayer graphene on the other AB-BLG, which thus consists of four graphene layers in total [Figs. 1(a) and 1(b)]. The resulting crystal structure has threefold rotation symmetry around the z axis, but lacks the inversion symmetry. The local stacking orders of TDBG vary across the moiré supercell. For instance, AB/AB , AB/BC and AB/CA stacking regions are denoted in the upper left plot of Fig. 1(c).

Preserving the crystal symmetries and the supercell lattice vectors, we determined equilibrium atomic positions of TDBG by minimizing the total energy U consisting of the in-plane elastic energy and the interlayer van der Waals binding energy (See Ref. [14] for the detailed description of the structural relaxation method). The

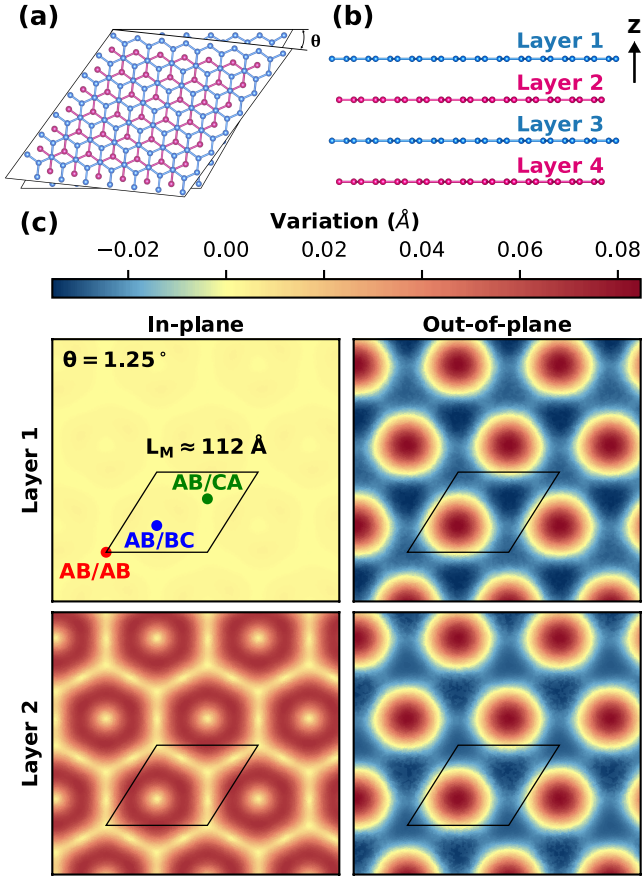


FIG. 1. Schematic (a) top and (b) side view of the twisted double bilayer graphene. (c) In-plane (left) and out-of-plane (right) variation of atomic positions in the first (top) and second (bottom) graphene layers after structure relaxation. The remaining two layers have similar variation patterns, except that atomic positions are varied in opposite directions.

in-plane elastic energy is calculated under the harmonic approximation where atomic force constants are considered up to the 4th nearest neighbors, as obtained by fitting *ab initio* phonon dispersion calculations [15]. The interlayer van der Waals binding energy is calculated using Kolmogorov-Crespi (KC) potential that depends on interlayer atomic registry [16]. Our method has been shown to be effective in obtaining relaxed atomic positions of magic-angle twisted bilayer graphene [14], and can be applied straightforwardly to twisted multilayer graphene systems.

The rotational mismatch at the interface of two bilayer graphene results in both in and out of plane variations of atomic positions. Figure 1(c) shows variations in the atomic positions of TDBG at $\theta = 1.25^\circ$ after the structural relaxation. The in-plane variation from the perfect honeycomb structure occur mostly for the inner two graphene layers and almost negligible in the outer two layers. In contrast, the out-of-plane variation is present in all of the four graphene layers. The interlayer dis-

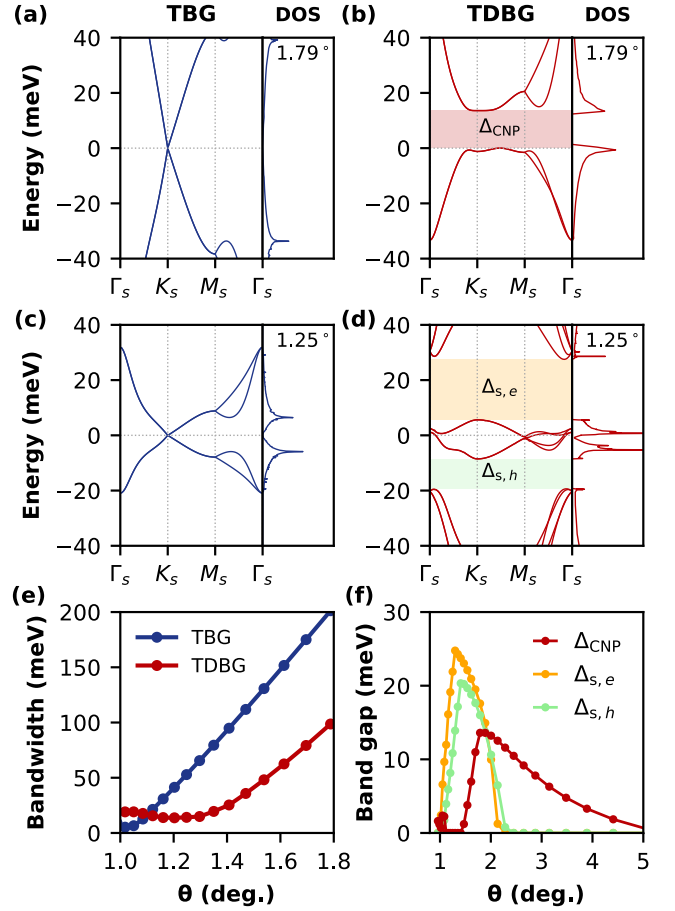


FIG. 2. Band structures and the density of states (DOS) of (a,c) twisted bilayer graphene and (b,d) twisted double bilayer graphene with relaxed atomic structures at twist angles of (a,b) 1.79° and (c,d) 1.25° . In (a-d), the absolute values of DOS are normalized to the same unit of states/meV/nm² so that their magnitudes can be directly compared. Plots of (a-d) in a wider energy range are given in Fig. S1 in the Supplemental Material [20]. (e) The bandwidths of the flat bands in TBG and TDBG as a function of the twist angle θ . (f) The band gap Δ_{CNP} at the charge neutral point and the band gap $\Delta_{s,e(h)}$ between the electron (hole)-side flat bands and higher (lower) energy bands as functions of θ in TDBG.

tance between the second and third layer, where the rotational mismatch is present, varies across the moiré supercell and is largest (smallest) at AB/BC (AB/CA) stacking regions. Atoms in the first layer relax vertically following the same out-of-plane displacement pattern of the second layer. Thus, the interlayer distance between the first and the second layer is nearly the same as that of AB-stacked bilayer graphene. Relaxation patterns of the third (fourth) layer are similar to those of the second (first) layer, except that they relax in the opposite direction.

With the relaxed atomic structures, we investigate the electronic structure of TDBG and compare it with TBG using an atomistic tight-binding approach [14, 17, 18].

Figures 2(a) and 2(b) show tight-binding band structures of TBG and TDBG at $\theta = 1.79^\circ$, respectively. At this angle, we note two important differences between the electronic structures of TBG and TDBG. First, the bandwidth of TDBG is much smaller than that of TBG at the same angle. Second, an intrinsic band gap (Δ_{CNP}) can open at the charge neutral point in TDBG, owing to the absence of the inversion symmetry. Notably, the valence and conduction band edges become extremely flat after the opening of Δ_{CNP} , and the electronic density of states is significantly enhanced near the band edges accordingly. The size of Δ_{CNP} can be as large as 13.6 meV, as shown in Fig. 2(f).

When we reduce the twist angle down to $\theta = 1.25^\circ$, TDBG shows nearly flat bands at the Fermi level while flat bands in TBG are more than two times wider [Figs. 2(c) and 2(d)]. The energy gap (Δ_{CNP}) at the charge neutral point is now closed at this angle because bands overlap in some parts of the Brillouin zone other than near the K_s point as a result of strong band flattening. The band splitting at the K_s point still exists, meaning that the effect of the inversion symmetry breaking persists. Similar to TBG [14, 19], the lattice relaxation in TDBG can open band gaps above the electron-side flat bands and below the hole-side flat bands, as denoted respectively by $\Delta_{s,e}$ and $\Delta_{s,h}$ in Fig. 2(d). The size of $\Delta_{s,e(h)}$ at this angle is about 21.9 (10.8) meV so that the flat bands in TDBG are well separated from the high energy bands.

In the Supplemental Material [20], Fig. S1 shows band structures of TBG and TDBG in a wider energy window, clearly showing $\Delta_{s,e(h)}$ in $\theta = 1.79^\circ$ and $\theta = 1.25^\circ$. Furthermore, in Fig. S2, we compare effects of the lattice relaxations on the electronic structure. In particular, we find that the size of the intrinsic band gap Δ_{CNP} does not depend on the relaxation.

Bandwidths and band gaps as functions of the twist angle are summarized in Figs. 2(e) and 2(f), respectively. The flat bands are generally narrower in TDBG than TBG for $\theta > 1.1^\circ$. The bandwidth in TDBG reaches a minimum value near $\theta = 1.25^\circ$, which can be regarded as the first magic angle of TDBG. The energy gap Δ_{CNP} in TDBG starts to develop near $\theta \sim 5^\circ$ and it reaches a maximum value of 13.6 meV at $\theta = 1.79^\circ$. Then Δ_{CNP} is closed near $\theta = 1.4^\circ$ and reopens below $\theta \sim 1.1^\circ$.

Now we investigate how a vertical electric field modifies the electronic structure of TDBG. We consider a vertical electric field by adding the following electrostatic energy term to the tight-binding Hamiltonian:

$$\Delta H = eE_z z, \quad (1)$$

where $e > 0$ is the elementary charge, E_z is the electric field strength, and z is the z -coordinates of atoms. Essentially the electric field makes on-site energy differences in each layer.

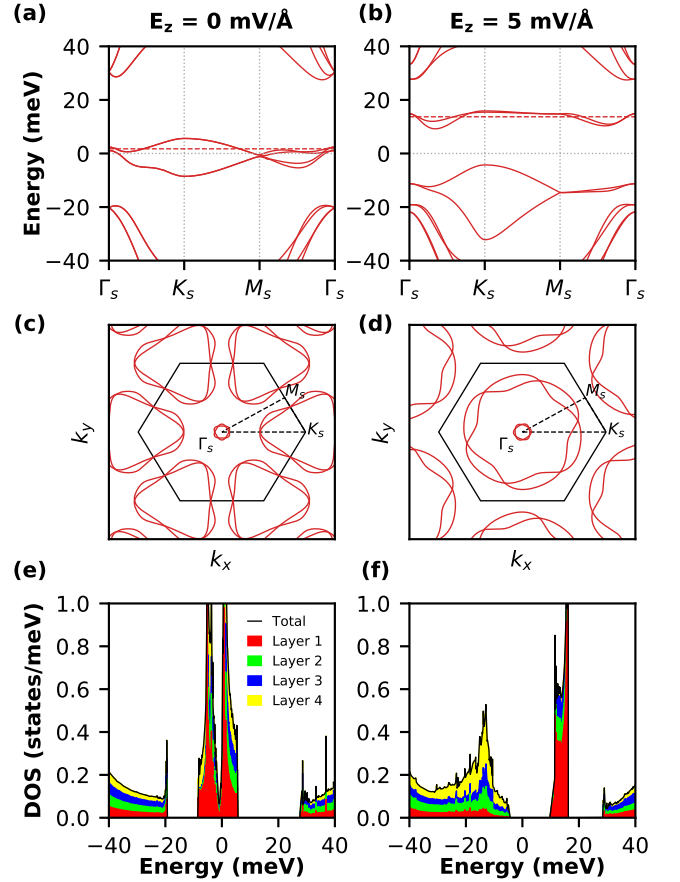


FIG. 3. Electronic structures of TDBG at $\theta = 1.25^\circ$. (a,b) Band structures with the vertical electric field E_z of (a) 0 mV/Å and (b) 5 mV/Å. Horizontal dashed lines denote half-filling energies of electron-side flat bands. (c,d) Fermi surfaces at the half-filling energies of the electron-side flat bands with E_z of (c) 0 mV/Å and (d) 5 mV/Å. (e,f) Electronic density of states with E_z of (e) 0 mV/Å and (f) 5 mV/Å. Contributions of the 1st, 2nd, 3rd, and 4th graphene layer to the total density of states are shown in red, green, blue, and yellow, respectively.

Figures 3(a) and 3(b) show the band structures at $\theta = 1.25^\circ$ with $E_z = 0$ and 5 mV/Å, respectively. Without the electric field, all of the four flat bands are present near the Fermi level and no band gap exists among them. When the vertical electric field of $E_z = 5$ mV/Å is applied, the flat bands are split into two groups and a band gap opens between them. Notably, the electron-side flat bands are much flatter than the hole-side flat bands, being separated from other bands. In contrast, the electric field makes the hole-side flat bands wider so they become overlapped in energy with the lower energy bands.

Fermi surfaces at half-filling energies of the flat bands are of special interest because correlation effects are often maximized at half-filling and TBG actually showed correlated insulating states at half-filling [4]. Figures 3(c) and 3(d) show Fermi surfaces in TDBG at the half-filling

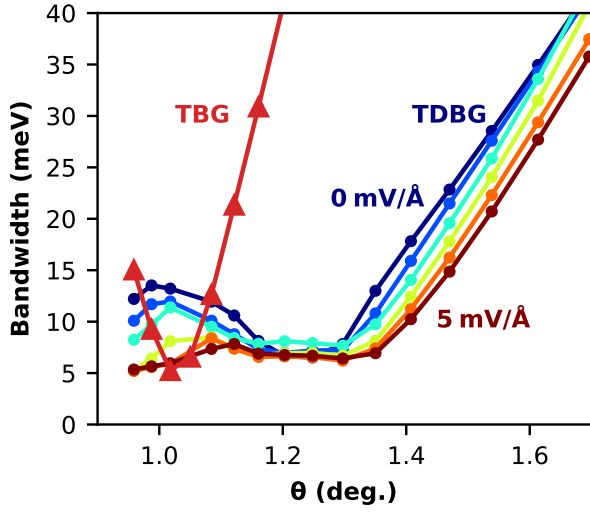


FIG. 4. Bandwidths of flat bands in TDBG at different twist angles θ and vertical electric fields E_z . Here E_z is increased from 0 to 5 mV/Å by a step of 1 mV/Å. For $E_z \geq 1$ mV/Å, bandwidths of the electron-side flat bands are plotted, which are separated from the hole-side ones. Bandwidths of the flat bands in TBG are also plotted for comparison.

of the electron-side flat bands without and with the electric field, respectively. The half-filling energy of each case is denoted by a dashed red line in Figs. 3(a) and 3(b). When the external electric field is not applied, two triangular hole pockets are located at corners of the Brillouin zone, and additional hole pockets exist near the Γ point [Fig. 3(c)]. When the electric field is applied, Fermi surfaces become more or less circular, and all the Fermi surfaces are centered at the Γ point [Fig. 3(d)].

The electric field also induces asymmetry in the layer distributions of the flat bands. Figure 3(e) shows the layer-projected density of states without the external electric field. The flat-band states are rather uniformly distributed over the four layers. However, the electric field along the $+z$ direction polarizes the flat-band states so that the electron (hole)-side flat bands become mostly confined within the first (fourth) layer. This effect is illustrated by the changes in the relative weights of each layer in the layer-projected density of states, as shown in Fig. 3(f). Along with such layer-polarization, the density of states is significantly enhanced for the electron-side flat bands. We expect that this large density of states, which are mainly localized in the first layer, would make correlation effects much stronger in the electron-side flat bands than the hole-side ones. For comparison, we also performed the same calculations using a nonrelaxed structure at the same twist angle $\theta = 1.25^\circ$, as shown in Fig. S3 in the Supplemental Material [20], where the flat bands in the nonrelaxed structure also show similar electrical tunability although they have slightly larger bandwidths and nonzero overlaps with high energy bands.

We elaborated more on the electrical tunability. Figure 4 shows the bandwidths of the flat bands as a function of the twist angle and the strength of the vertical electric field. Without the electric field, the bandwidth of TDBG reaches the minimum value at the twist angle of $\theta \sim 1.25^\circ$ and then increases again as the twist angle is further lowered [Figs. 2(e) and 4]. When the electric field is applied, the bandwidth of TDBG is continuously reduced for the most of twist angles (Fig. 4). For all the twist angles in the range of $\theta = 0.96 \sim 1.4^\circ$, applied electric fields can make the bandwidth of the electron-side flat bands smaller than 10 meV, which is similar to the minimum bandwidth that can be obtained at the magic-angle twisted bilayer graphene. This strongly suggests that correlated electron physics can emerge in TDBG in a wide range of the twist angle rather than at certain special magic angles. We also calculated the electronic structure of TBG under the external electric field and obtained that the electric-field strength considered in our present work has almost negligible effects in the TBG case, which is consistent with a previous study [21]. Thus, the strong tunability of the bandwidth with the external electric field is a very distinctive feature of TDBG compared with TBG.

In conclusion, we have performed atomistic calculations for the atomic and electronic structures of twisted double bilayer graphene. In the equilibrium atomic structures, in-plane strain is present mainly at the rotationally mismatched interface, while the out-of-plane relaxation is significant in all of the four graphene layers. Since the crystal structure lacks the inversion symmetry, the electronic structure of TDBG can have an intrinsic band gap at the charge neutral point over a large range of the twist angle. At low twist angles, TDBG hosts well-isolated flat bands near the Fermi level, which are generally narrower than the flat bands in TBG for $\theta > 1.1^\circ$. Furthermore, we have shown that, by applying a vertical electric field, the low-energy electronic structure of TDBG can be easily tuned, and extremely narrow bands can be obtained in the electron side in a wide range of the twist angle, suggesting bigger chance of correlated electronic states. Our results provide basic electronic structures that serve as a guide for exploring emergent correlated electron physics, and illustrate the importance of the layer-number degree of freedom in tailoring flat-band physics in moiré superlattices.

This work was supported by NRF of Korea (Grant No. 2011-0018306). Y.W.C. acknowledges support from NRF of Korea (Global Ph.D. Fellowship Program NRF-2017H1A2A1042152). Computational resources have been provided by KISTI Supercomputing Center (Project No. KSC-2018-CRE-0097).

* h.j.choi@yonsei.ac.kr

- [1] T. de Laissardi re, D. Mayou, and L. Magaud, Localization of Dirac Electrons in Rotated Graphene Bilayers, *Nano Lett.* **10**, 804 (2010).
- [2] E. S. Morell, J. D. Correa, P. Vargas, M. Pacheco, and Z. Barticevic, Flat bands in slightly twisted bilayer graphene: Tight-binding calculations, *Phys. Rev. B* **82**, 121407 (2010).
- [3] R. Bistritzer and A. MacDonald, Moir  bands in twisted double-layer graphene, *Proc. Natl. Acad. Sci. U.S.A.* **108**, 12233 (2011).
- [4] Y. Cao, V. Fatemi, A. Demir, S. Fang, S. L. Tomarken, J. Y. Luo, J. D. Sanchez-Yamagishi, K. Watanabe, T. Taniguchi, E. Kaxiras, R. C. Ashoori, and P. Jarillo-Herrero, Correlated insulator behaviour at half-filling in magic-angle graphene superlattices, *Nature (London)* **556**, 80 (2018).
- [5] Y. Cao, V. Fatemi, S. Fang, K. Watanabe, T. Taniguchi, E. Kaxiras, and P. Jarillo-Herrero, Unconventional superconductivity in magic-angle graphene superlattices, *Nature (London)* **556**, 43 (2018).
- [6] S. Carr, S. Fang, P. Jarillo-Herrero, and E. Kaxiras, Pressure Dependence of the Magic Twist Angle in Graphene Superlattices, *Phys. Rev. B* **98**, 085144 (2018).
- [7] B. L. Chittari, N. Leconte, S. Javvaji, and J. Jung, Pressure induced compression of flatbands in twisted bilayer graphene, *Electron. Struct.* **1**, 015001 (2019).
- [8] M. Yankowitz, S. Chen, H. Polshyn, Y. Zhang, K. Watanabe, T. Taniguchi, D. Graf, A. F. Young, and C. R. Dean, Tuning Superconductivity in Twisted Bilayer Graphene, *Science*, eaav1910 (2019).
- [9] T. Ohta, A. Bostwick, T. Seyller, K. Horn, and E. Rotenberg, Controlling the Electronic Structure of Bilayer Graphene, *Science* **313**, 951-954 (2006).
- [10] E. V. Castro, K. S. Novoselov, S. V. Morozov, N. M. R. Peres, J. M. B. Lopes dos Santos, J. Nilsson, F. Guinea, A. K. Geim, and A. H. Castro Neto, Biased Bilayer Graphene: Semiconductor with a Gap Tunable by the Electric Field Effect, *Phys. Rev. Lett.* **99**, 216802 (2007).
- [11] Y. Zhang, T.-T. Tang, C. Girit, Z. Hao, M. C. Martin, A. Zettl, M. F. Crommie, Y. R. Shen, and F. Wang, Direct Observation of a Widely Tunable Bandgap in Bilayer Graphene, *Nature* **459**, 820 (2009).
- [12] Y.-H. Zhang, D. Mao, Y. Cao, P. Jarillo-Herrero, and T. Senthil, Nearly flat Chern bands in moir  superlattices, *Phys. Rev. B* **99**, 075127 (2019).
- [13] N. R. Chebrolu, B. L. Chittari, and J. Jung, Flatbands in twisted bi-bilayer graphene, *arXiv:1901.08420* (2019).
- [14] Y. W. Choi and H. J. Choi, Strong electron-phonon coupling, electron-hole asymmetry, and nonadiabaticity in magic-angle twisted bilayer graphene, *Phys. Rev. B* **98**, 241412(R) (2018).
- [15] L. Wirtz and A. Rubio, The Phonon Dispersion of Graphite Revisited, *Solid State Commun.* **131**, 141 (2004).
- [16] A. N. Kolmogorov and V. H. Crespi, Registry-dependent interlayer potential for graphitic systems, *Phys. Rev. B* **71**, 235415 (2005).
- [17] P. Moon and M. Koshino, Energy spectrum and quantum Hall effect in twisted bilayer graphene, *Phys. Rev. B* **85**, 195458 (2012).
- [18] T. Nakanishi and T. Ando, Conductance of crossed carbon nanotubes, *J. Phys. Soc. Jpn.* **70**, 1647 (2001).
- [19] N. N. T. Nam and M. Koshino, Lattice relaxation and energy band modulation in twisted bilayer graphene, *Phys. Rev. B* **96**, 075311 (2017).
- [20] See Supplemental Material for (i) comparison of electronic structures of TBG and TDBG for a wider energy range than in Fig. 2, (ii) effects of atomic-position relaxation on electronic structures of TDBG, and (iii) electronic structures of nonrelaxed TDBG under electric fields.
- [21] P. Moon, Y.-W. Son and M. Koshino, Optical absorption of twisted bilayer graphene with interlayer potential asymmetry, *Phys. Rev. B* **90** 155427 (2014).

Supplemental Material: Intrinsic Band Gap and Electrically Tunable Flat Bands in Twisted Double Bilayer Graphene

Young Woo Choi and Hyoungh Joon Choi*

Department of Physics, Yonsei University, Seoul 03722, Korea

(Dated: March 5, 2019)

This supplemental material provides (i) comparison of electronic structures of twisted bilayer graphene and twisted double bilayer graphene (TDBG) for a wider energy range than in Fig. 2 in the main text, (ii) effects of atomic-position relaxation on electronic structures of TDBG, and (iii) electronic structures of nonrelaxed TDBG under electric fields.

Figure S1 shows electronic structures of twisted bilayer graphene (TBG) and twisted double bilayer graphene (TDBG) with relaxed atomic positions at twisted angles of $\theta = 1.79^\circ$ and 1.25° , plotted for a wider energy range than in Fig. 2 in the main text. Bandwidths of narrow bands near zero energy in TDBG are about half of those in TBG. In both TBG and TDBG, band gaps are clearly present above and below the narrow bands. At $\theta = 1.25^\circ$, the density of states (DOS) shows multiple strong peaks at high energies as well as near flat-band energies.

Figure S2 shows electronic structures of TDBG at different twist angles before and after atomic-position relaxation.

Firstly, the band gap at the charge neutral point is present both before and after the relaxation at $\theta = 3.15^\circ$ and 1.79° , and the size of the band gap is almost unaffected by the relaxation. Bandwidths of narrow bands near zero energy are not affected significantly by the relaxation, either. Secondly, below $\theta \sim 2^\circ$, energy gaps open above and below the narrow bands after the relaxation, which become more pronounced as θ is lowered.

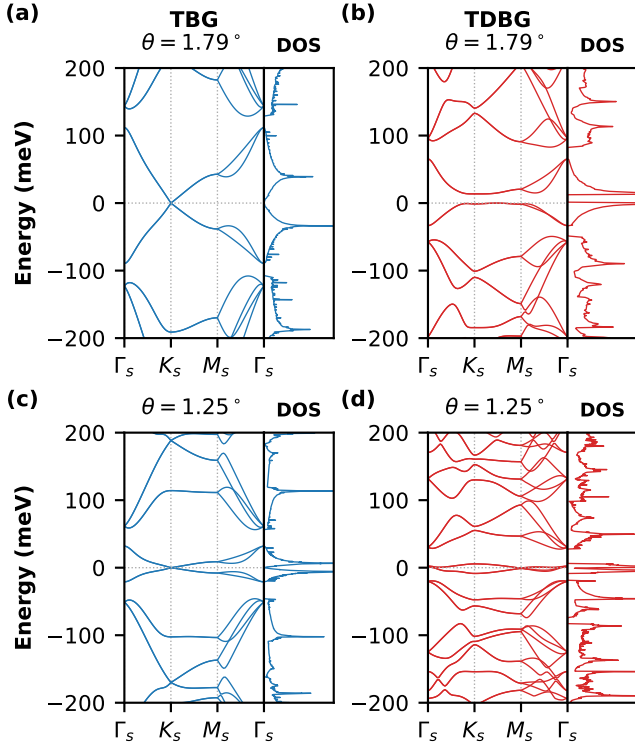


FIG. S1. Electronic structures of (a,c) TBG and (b,d) TDBG with relaxed atomic positions at (a,b) $\theta = 1.79^\circ$ and (c,d) $\theta = 1.25^\circ$. Electronic band structures and DOS are plotted for a wider energy range than in Fig. 2. In all cases, very narrow bands appear near zero energy and band gaps are clearly shown above and below the narrow bands.

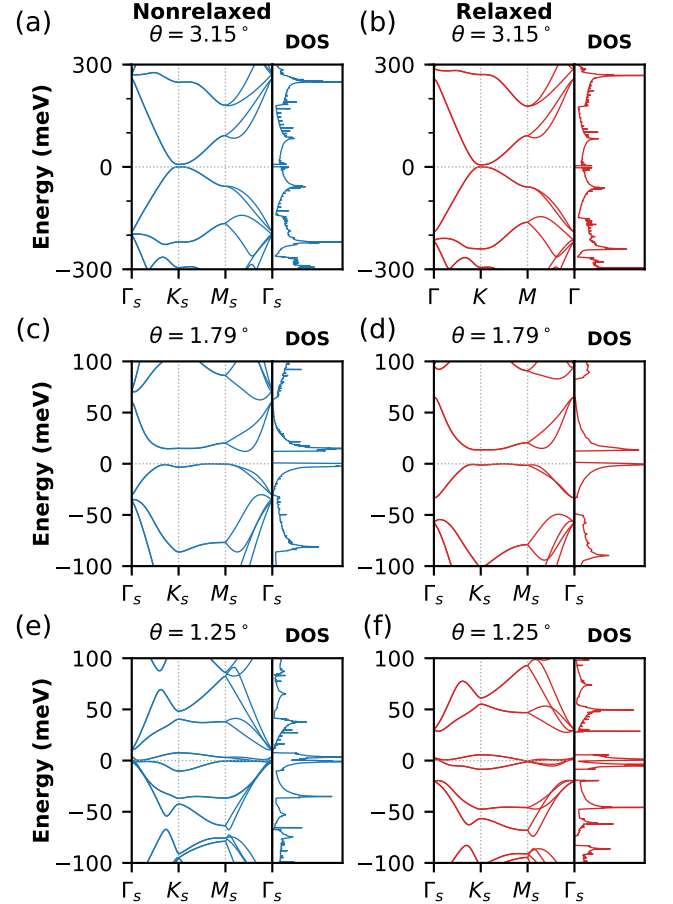


FIG. S2. Band structures of TDBG with (a,c,e) nonrelaxed and (b,d,f) relaxed atomic positions at twist angles of (a,b) 3.15° , (c,d) 1.79° , and (e,f) 1.25° . Effects of atomic-position relaxation become more important as the twist angle is lowered.

Figure S3 shows electronic structures of nonrelaxed TDBG under electric fields. Compared with the case of relaxed TDBG shown in Fig. 3 in the main text, band dispersions of flat bands and Fermi surfaces at the half-filling energies are generically similar. However, without atomic-position relaxation, flat bands have wider bandwidths and they are not clearly separated from high energy bands.

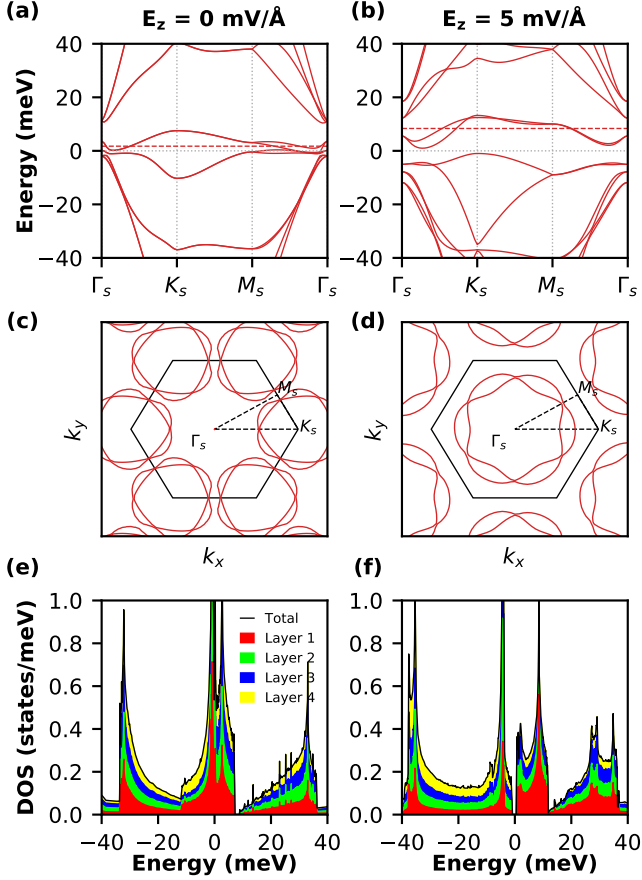


FIG. S3. Electronic structures of TDBG with *nonrelaxed* atomic positions at $\theta = 1.25^\circ$. (a,b) Band structures with the vertical electric field E_z of (a) 0 mV/Å and (b) 5 mV/Å. Horizontal dashed lines denote half-filling energies of electron-side flat bands. (c,d) Fermi surfaces at the half-filling energies of the electron-side flat bands with E_z of (c) 0 mV/Å and (d) 5 mV/Å. (e,f) Electronic density of states with E_z of (e) 0 mV/Å and (f) 5 mV/Å. Contributions of the 1st, 2nd, 3rd, and 4th graphene layer to the total density of states are shown in red, green, blue, and yellow, respectively.